



Thermal evolution of neutron stars  
by Letao Qin

A thesis submitted in partial fulfillment of the requirements for the degree of Doctor of Philosophy in  
Physics  
Montana State University  
© Copyright by Letao Qin (1995)

Abstract:

The neutron star thermal calculation is to simulate how temperatures of neutron stars will evolve with time. The ultrahigh density of neutron stars ( $10^{15} \text{g cm}^{-3}$ ) is a physical condition that cannot be realized in a laboratory so far, and that implies serious theoretical difficulties. Our work on neutron star thermal evolution is to calculate the cooling history of the star and to eliminate some theoretical uncertainties by comparing with the observational data. Among them, the thermal effects of strong magnetic fields, crust breaking, axion emission and neutrino magnetic dipole moment are the four projects we have worked on.

The results we obtained are encouraging for all four cases. We found that a magnetic neutron star will maintain a relatively high temperature for a period longer than a non-magnetic star. In the case of crust breaking, our calculations show that for an ideal lattice, the heating due to crust breaking is significant, while for an imperfect lattice, it is not. By including axion emission and effects of neutrino magnetic dipole moment into the neutron star cooling calculations and by comparing with the observational data, we are able to obtain limits on some theoretical parameters, i.e. the mass of axions and neutrino magnetic dipole moment.

Also we developed a new way to connect theoretical calculations and observational data through light curves. Theoretical constructions of light curves and comparison with observational data enable us to determine the configurations of magnetic fields and the mechanisms of the emission near the surface of neutron stars.

THERMAL EVOLUTION OF NEUTRON STARS

by  
Letao Qin

A thesis submitted in partial fulfillment  
of the requirements for the degree  
of  
Doctor of Philosophy  
in  
Physics

MONTANA STATE UNIVERSITY  
Bozeman, Montana

December 1995

D378  
Q16

APPROVAL

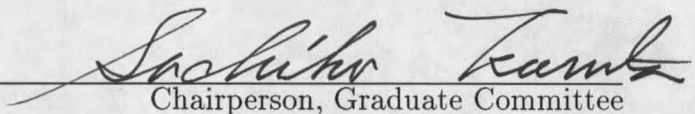
of a thesis submitted by

Letao Qin

This thesis has been read by each member of the thesis committee and has been found to be satisfactory regarding content, English usage, format, citations, bibliographic style, and consistency, and is ready for submission to the College of Graduate Studies.

12/1/95

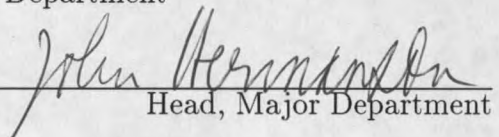
Date

  
Chairperson, Graduate Committee

Approved for the Major Department

12-1-95

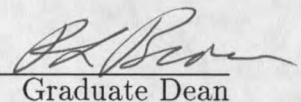
Date

  
Head, Major Department

Approved for the College of Graduate Studies

12/20/95

Date

  
Graduate Dean

## STATEMENT OF PERMISSION TO USE

In presenting this thesis in partial fulfillment of the requirements for a doctoral degree at Montana State University, I agree that the Library shall make it available to borrowers under rules of the Library. I further agree that copying of this thesis is allowable only for scholarly purposes, consistent with "fair use" as prescribed in the U.S. Copyright Law. Requests for extensive copying or reproduction of this thesis should be referred to University Microfilms International, 300 North Zeeb Road, Ann Arbor, Michigan 48106, to whom I have granted "the exclusive right to reproduce and distribute my dissertation in and from microform, along with the non-exclusive right to reproduce and distribute my abstract in any format in whole or in part."



Signature

Date Dec. 3, 1995

## ACKNOWLEDGMENTS

The author wants to thank Dr. Tsuruta for the guidance she has provided during the course of this research; Dr. Tsuruta and Dr. Link for their careful review of this thesis and valuable suggestions, and the members of my committee (Dr. Tsuruta, Dr. Lindblom, Dr. Link, Dr. Hermanson & Dr. Cone) for their support.

Thanks are also due to the physics department. Without the precious opportunity it offered to me and its excellent research environment, the work here would not have been possible.

## TABLE OF CONTENTS

	Page
1. INTRODUCTION .....	1
1.1 DISCOVERY OF PULSARS .....	2
1.2 STRUCTURE OF NEUTRON STARS .....	7
1.2.1 Basic Equations .....	7
1.2.2 Equation of State .....	8
1.2.3 Density Profile .....	12
1.3 MAGNETIC FIELD AND SUPERFLUIDITY .....	16
1.3.1 Magnetic Fields .....	16
1.3.2 Superfluidity .....	22
2. ONE DIMENSIONAL COOLING CALCULATION .....	32
2.1 INTRODUCTION .....	32
2.2 METHOD OF NEUTRON STAR COOLING CALCULATIONS .....	35
2.2.1 Isothermal Method .....	35
2.2.2 Exact Evolutionary Method .....	39
2.3 PHYSICAL INPUT .....	47
2.3.1 Equation of State & Specific Heat .....	47
2.3.2 Neutrino Emissivity .....	54
2.3.3 Opacity .....	62
2.4 EFFECTS OF MAGNETIC FIELDS ON OPACITY .....	64
2.4.1 General Consideration .....	64
2.4.2 Heat Transport under Strong Magnetic Fields .....	71
2.4.3 Radiative Conductivity .....	74
2.4.4 Electron Conductivity .....	75
2.4.5 Effects of Magnetic Fields on 1D Cooling .....	77
2.5 RESULTS FROM 1D COOLING CALCULATIONS .....	80

TABLE OF CONTENTS — Continued

	Page
2.6 DISCUSSIONS .....	83
3. TWO DIMENSIONAL COOLING CALCULATION .....	91
3.1 INTRODUCTION .....	91
3.2 TWO-DIMENSIONAL EVOLUTIONAL EQUATIONS .....	94
3.3 NUMERICAL METHOD .....	96
3.4 RESULTS AND DISCUSSIONS .....	105
4. HEATING OF NEUTRON STARS BY CRUST BREAKING .....	111
4.1 INTRODUCTION .....	111
4.2 PHYSICAL INPUTS .....	114
4.3 RESULTS .....	118
4.3.1 Heating due to Crust Breaking .....	118
4.3.2 Thermal Impulses .....	125
5. NEUTRON STARS AS A PLAYGROUND .....	137
5.1 AXION EMISSION .....	138
5.1.1 Introduction .....	138
5.1.2 Axion Emissivity .....	139
5.1.3 Results .....	147
5.1.4 Discussions .....	153
5.2 NEUTRINO MAGNETIC DIPOLE MOMENT .....	154
5.2.1 General Considerations .....	154
5.2.2 Constraints from Neutron Star Cooling .....	157
5.2.3 Discussions .....	164

TABLE OF CONTENTS — Continued

	Page
6. THERMAL X-RAY OBSERVATION OF NEUTRON STARS .....	166
6.1 INTRODUCTION .....	166
6.2 X-RAY TELESCOPE .....	167
6.3 DATA ANALYSIS OF PSR0656+14 .....	173
6.3.1 Spatial Analysis .....	173
6.3.2 Timing Analysis .....	175
6.3.3 Spectral Analysis .....	177
6.4 THEORETICAL LIGHT CURVES AND COMPARISON WITH OBSERVATION .....	182
7. CONCLUSION .....	190
BIBLIOGRAPHY .....	195
APPENDICES .....	201
A. COEFFICIENTS $A_{i,j}$ AND $F_{i,j}$ IN 1D CALCULATION .....	202
B. COEFFICIENTS $\Xi$ , $\mu$ , $\alpha$ AND $\beta$ IN 2D CALCULATION .....	204
C. MATRIX INVERSION CODE IN 2D CALCULATION .....	206
D. DERIVATION OF AXION EMISSIVITY $\epsilon_{ann}$ .....	214

## LIST OF TABLES

Table	Page
2.1 Compositions of Neutron Star Matter .....	51
2.2 Equation of State for the FP, PS, BPS Models .....	55
4.1 Size of the Crust Region of Different Ages (the FP Model) .....	117
5.1 Luminosity Function of Hyades Cluster .....	156
6.1 Photon Event File .....	174
6.2 Detection of Pulsars .....	183

## LIST OF FIGURES

Figure	Page
1.1 Density Profile for FP Type Neutron Stars .....	13
1.2 Density Profile for PS Type Neutron Stars .....	14
1.3 Density Profile for BPS Type Neutron Stars .....	15
1.4 Illustration of a Dipolar Magnetic Field .....	23
1.5 Solution of $f(E) = \sum_{p_1 p_2} V_0 / \frac{p_1^2 + p_2^2}{2m} - E$ .....	27
1.6 Effects of Superfluidity on Neutron Star Cooling, the FP Model .....	31
2.1 Cooling Profile from Isothermal Method .....	36
2.2 $T_c$ vs. $t$ ( zero field ) .....	38
2.3 Mesh in 1D Calculation .....	42
2.4 Surface Pressure vs. Surface Temperature .....	48
2.5 Structures of the Envelope .....	49
2.6 Emissivity of Modified URCA Process .....	59
2.7 Emissivity of Bremsstrahlung Process .....	60
2.8 Emissivity of Plasmon Neutrino Process .....	61

LIST OF FIGURES — Continued

Figure	Page
2.9 Total Opacity $\kappa$ vs. Density $\rho$ .....	65
2.10 Cooling Curves of the FP, PS, BPS Models .....	66
2.11 Cooling of Neutron Stars with Uniform Fields .....	81
2.12 Cooling of Neutron Stars with Dipolar Fields .....	82
2.13 $T/T_{pole}$ vs. Magnetic Colatitude .....	84
2.14 $T_c$ vs. $t$ ( equatorial ) .....	86
2.15 Total Luminosity of Magnetic ( 1D ) and Non-Magnetic Neutron Stars .....	87
2.16 Polar and Equatorial Core Temperatures, 1D Calculation .....	89
3.1 2D Mesh .....	92
3.2 2D Linear Equations .....	103
3.3 Cooling of Magnetic Neutron Stars, ( 2D Calculation ) .....	106
3.4 Core Temperature from 2D Calculation .....	108
3.5 Total Luminosity of Magnetic ( 2D ) and Non-Magnetic Neutron Stars .....	109

LIST OF FIGURES — Continued

Figure	Page
4.1 Heating by Crust Breaking, the FP Model .....	119
4.2 Heating by Crust Breaking, the PS Model .....	120
4.3 Heating by Crust Breaking, the BPS Model .....	121
4.4 Non-Standard Cooling with Crust Breaking Heating Effect .....	123
4.5 Non-Standard Cooling with Superfluidity ( No Heating ) .....	126
4.6 Superfluid Model E1 with Crust Breaking Heating .....	127
4.7 Superfluid Model E2 with Crust Breaking Heating .....	128
4.8 Superfluid Model AO with Crust Breaking Heating .....	129
4.9 Superfluid Model E1-0.3 with Crust Breaking Heating .....	130
4.10 Superfluid Model E1-0.5 with Crust Breaking Heating .....	131
4.11 Thermal Impulses of Different Energy Depositions .....	133
4.12 Thermal Impulses Taking Place at Different Ages, $\text{Log}(E) = 48.3\text{erg}$ .....	134
4.13 Thermal Impulses Taking Place at Different Regions, $\text{Log}(E) = 48.3\text{erg}$ ...	136
5.1 Feynman Diagram of Axion nn Bremsstrahlung Process .....	141

LIST OF FIGURES — Continued

Figure	Page
5.2 Function $F(x)$ and $G(y)$ .....	143
5.3 Feynman Diagram of Axion np Bremsstrahlung Process .....	144
5.4 $\epsilon_a$ vs. $\rho$ at $T = 10^9, 10^8, 10^7 K$ .....	148
5.5 Cooling with Axion Emission, the FP Model .....	150
5.6 Cooling with Axion Emission, the PS Model .....	151
5.7 Cooling with Axion Emission, the BPS Model .....	152
5.8 Effects of Neutrino Magnetic Dipole Moment on Cooling, the FP Model .....	160
5.9 Effects of Neutrino Magnetic Dipole Moment on Cooling, the PS Model .....	161
5.10 Effects of Neutrino Magnetic Dipole Moment on Cooling, the BPS Model .....	162
6.1 Observed Light Curve for Vela Pulsar .....	168
6.2 Wolter Type 1 Mirror .....	170

LIST OF FIGURES — Continued

Figure	Page
6.3 PSR0656+14 .....	176
6.4 Light Curve of PSR0656+14 .....	178
6.5 Spectral Analysis for PSR0656+14 (i) .....	180
6.6 Spectral Analysis for PSR0656+14 (ii) .....	181
6.7 Illustration of a Observational Scene .....	184
6.8 Geometry of a Photon Path near the Surface of a Neutron Star .....	184
6.9 Theoretical Light Curves for Vela Pulsar .....	189

## ABSTRACT

The neutron star thermal calculation is to simulate how temperatures of neutron stars will evolve with time. The ultrahigh density of neutron stars ( $10^{15} g cm^{-3}$ ) is a physical condition that cannot be realized in a laboratory so far, and that implies serious theoretical difficulties. Our work on neutron star thermal evolution is to calculate the cooling history of the star and to eliminate some theoretical uncertainties by comparing with the observational data. Among them, the thermal effects of strong magnetic fields, crust breaking, axion emission and neutrino magnetic dipole moment are the four projects we have worked on.

The results we obtained are encouraging for all four cases. We found that a magnetic neutron star will maintain a relatively high temperature for a period longer than a non-magnetic star. In the case of crust breaking, our calculations show that for an ideal lattice, the heating due to crust breaking is significant, while for an imperfect lattice, it is not. By including axion emission and effects of neutrino magnetic dipole moment into the neutron star cooling calculations and by comparing with the observational data, we are able to obtain limits on some theoretical parameters, i.e. the mass of axions and neutrino magnetic dipole moment.

Also we developed a new way to connect theoretical calculations and observational data through light curves. Theoretical constructions of light curves and comparison with observational data enable us to determine the configurations of magnetic fields and the mechanisms of the emission near the surface of neutron stars.

# Chapter 1

## Introduction

The possible existence of neutron stars was first proposed by Walte Baade and Fritz Zwicky in 1934 (1934). A little more than 30 years later, radio pulsars were discovered in Cambridge by Anthony Hewlish and Jocelyn Bell (1968). Because of the peculiar property of neutron stars, ultrahigh density ( $10^{15} g cm^{-3}$ ), theoretical uncertainties, such as the equation of state of matters with density higher than nucleon density, the effect of magnetic fields, the presence of exotic particles, e.g. axion, pion, kaon, etc, are overwhelming. Fortunately modern X-ray satellites have been able to observe X-ray pulsars, and to some degree, the observational data helps us eliminate the theoretical uncertainties.

My PhD research projects are neutron star thermal evolution calculations. In Chapter 1, I will give a brief introduction to the study of neutron stars. In Chapters 2 and 3, I will present our simulations of the thermal evolution of magnetized neutron stars. In Chapter 4 and Chapter 5, I will introduce several examples of how particle and solid state theories are tested in the neutron star laboratory, mainly three projects

we worked on: starquakes, neutrino magnetic dipole moment and axion emissions. In Chapters 2 through 5, the validity and uncertainty of theoretical predictions are discussed by comparing with observational data. In Chapter 6, I will describe the current status of X-ray observations of pulsars and demonstrate how theoretical light curve calculations are able to determine the observational parameters.

In this chapter, section §1.1 summarize the discovery of neutron stars. Section §1.2 describes neutron star interior. In section §1.3, we discuss neutron star magnetic fields and the possible existence of superfluid in the interior.

## 1.1 Discovery of Pulsars

At the beginning of this century, it gradually became clear to physicists that the Sun is powered by nuclear reactions. One of the basic nuclear reactions inside a star is  $4H \rightarrow He + \gamma + \nu$ . Once the mechanism by which stars shine was understood, the question that naturally followed was: what would happen to the stars when their main fuel, hydrogen, was exhausted? One possibility is that the star becomes a white dwarf. The first white dwarf, Sirius B, was discovered by W.S. Adams in 1914 (1915). Sirius B has very high density. Its mass is about 1 solar mass, its radius is only about 20,000 km,  $10^{-2}$  of the radius of the sun ( $R_{\odot} = 7 \times 10^5 \text{km}$ ). The average density of white dwarfs is  $10^7 \text{gcm}^{-3}$ . In ordinary stars, the pressure resulting from collisions maintains hydrostatic equilibrium. In white dwarfs, the density is so high that the pressure required to balance gravity is tremendous, impossible to be explained by ideal gas law.

In 1926, Fowler solved this puzzle by applying Fermi-Dirac statistics to the electrons inside neutron stars. Because electrons are fermions, their distribution satisfies the Fermi-Dirac function. When the number density  $n$  is large, the electrons will be forced to populate high energy levels. These electrons at high energy levels have large velocities, and the pressure provided by such electrons provides the major part of the pressure required to balance gravity.

In 1932, Chadwick discovered neutrons. Neutrons are fermions, have spin  $\frac{1}{2}$  and no charge. In 1932, after he learned about the discovery of neutrons, Landau (1932) applied Fermi-Dirac statistics to "neutron stars", stars supposed to consist primarily of neutrons, and obtain a mass limit for neutron stars. In 1934, Walter Baade and Fritz Zwicky proposed the idea that neutron stars would be the end point of stellar evolution. In their paper, they wrote:

*with all reserve we advance the view that a supernovae represents the transition of an ordinary star into a neutron star, consisting mainly of neutrons. Such a star may possess a very small radius and an extremely high density.*

It seemed impossible to confirm such a claim at that time. Only some 30 years later, when neutron stars astoundingly presented themselves as radio pulsars, the idea of neutron stars began to be accepted by astrophysicists.

Nevertheless during those years, some pioneer theoretical calculations on neutron stars were carried out. Oppenheimer and Volkoff (1939) first calculated the structure of neutron stars. Their calculations showed that a neutron star could have a central density as high as  $10^{15} \text{gcm}^{-3}$  when the mass of the neutron star is about 0.7 solar

mass. Following that, Harrison, Wakano and Wheeler (1958), Cameron (1959a), Ambartsumyan and Saakyan (1960), and Hamada and Salpeter (1961) discussed in detail the equation of state and neutron star models. Tsuruta (1964) first carried out thermal evolution calculations of neutron stars. A neutron star is a product of supernova explosion. When it is born, its temperature is very high, above 1 MeV. Afterwards, it is cooled by neutrino emission and photon emission. In her thesis, Tsuruta calculated how the surface temperatures of neutron stars would evolve with time.

In 1967, Hewlish, a radio astronomer, and his student Bell at Cambridge discovered an extremely regular pulse series. The period of the signal was about 1.377 seconds. In their paper (1968), they pointed out that the radio signal must be from outside the solar system and that the rapidity of the pulsation showed that the source must be very small, probably a condensed star, presumably either a white dwarf or a neutron star. The identity of radio pulsars as neutron stars was soon established by Gold (1968).

When the cause of pulsating is mechanical, the fundamental physical quantities describing such a system would be the total mass  $M$  and density  $\rho$  of this system. The characteristic dynamical time  $\tau$  should be:

$$\tau \propto (G\rho)^{-2} \quad (1.1)$$

If  $\tau$  is  $\sim 0.1$  second,  $\rho$  would be  $\sim 10^{12} \text{gcm}^{-3}$ . This density is much higher than the densities of all known objects at that time. The average density of a white dwarf is only  $10^7 \text{gcm}^{-3}$ , far smaller than  $10^{12} \text{gcm}^{-3}$ , while an ordinary star has  $\rho \sim 1 \text{gcm}^{-3}$ .

But according to the calculations of Oppenheimer and Volkoff, neutron stars could have densities as high as  $10^{15} \text{gcm}^{-3}$ .

If the pulsar is a neutron star, how are the radio signals produced? Gold (1968) suggested that the radio signals from a neutron star are caused by the magnetic fields around the star. When a neutron star is rotating, carrying a strong dipolar magnetic field with it, it acts as a very energetic electric generator, and provides a source of energy for radiation. The radiation from a rotating dipole is

$$\frac{dE}{dt} = \frac{2}{3c^3} \left| \frac{d^2 \vec{m}}{dt^2} \right|^2, \quad (1.2)$$

where  $\vec{m}$  is the magnetic dipole moment. For a rotating dipolar field,  $|\vec{m}| = B_p R^3 / 2$ ,  $d\vec{m}/dt$  is

$$\frac{d\vec{m}}{dt} = \vec{m} \times \vec{\Omega} \sim \frac{B_p R^3}{2} \Omega \sin \alpha, \quad (1.3)$$

with  $\vec{\Omega}$  as the angular velocity,  $\alpha$  the angle between  $\vec{m}$  and  $\vec{\Omega}$ , and

$$\frac{d^2 \vec{m}}{dt^2} = \frac{B_p R^3}{2} \Omega^2 \sin^2 \alpha. \quad (1.4)$$

So

$$\frac{dE}{dt} = \frac{B_p^2 R^6 \Omega^4}{6c^3} \sin^4 \alpha. \quad (1.5)$$

Since the energy is being lost, Gold predicted that the rotation period of the neutron star will increase and the rate of increase would be:

$$\frac{d(\frac{1}{2} I \Omega^2)}{dt} = -\dot{E}, \quad (1.6)$$

so that,

$$I \Omega \dot{\Omega} = -\dot{E}, \quad (1.7)$$

$$\dot{\Omega} = -\frac{\dot{E}}{I\Omega} = -\frac{B_p^2 R^6 \Omega^3}{6c^3 I} \sin^4 \alpha. \quad (1.8)$$

In 1975, when the Crab Pulsar was discovered, a slow increase of the period was detected. At that time, the period of the Crab Pulsar was 33ms, and the rate of increase of the period was  $dP/dt = 1.2589 \times 10^{-15}$ . If we assume this increase of the period is due to the radiation of the magnetic dipole, then  $B_p$  should be about  $5 \times 10^{12}G$ . Thus, the increase of the period of the Crab pulsar suggests the presence of strong magnetic fields associated with neutron stars. Further evidence, the emission line from HerX-1, will be discussed in §1.3.

With their ultrahigh densities, neutron stars have been attracting attentions of physicists. Neutron stars have become a testing ground for nuclear, particle and solid state theories. Different theories can be incorporated into the thermal calculation of neutron stars, and compared with the observational data in order to be tested.

By now neutron stars are not only being observed through radio telescopes, but also in X-rays and Gamma-rays. Even before the discovery of radio pulsars, a rocket-borne X-ray experiment on board observed Sco X-1, a powerful X-ray source. This X-ray source is now known to be a binary star system. One member of this binary system is a neutron star, and X-rays come from the accretion of materials from an ordinary star onto the neutron star. Later with X-ray satellites, such as UHURU, Einstein and ROSAT, more and more pulsars are studied in the X-ray range. The surface temperatures of these pulsars then can be deduced from the flux intensity and spectrum of the soft X-rays from the surfaces of neutron stars, and comparisons between the observational data and theoretical thermal calculations can be made.

Such comparisons are necessary in order to make judgement on several alternative theories.

## 1.2 Structure of Neutron Stars

### 1.2.1 Basic Equations

The mass of a neutron star is usually around 1 solar mass, and the radius of a neutron star is about 10 km, about 10 times the Schwarzschild radius. Hence general relativistic effects are relevant in determining the star's structure.

The hydrostatic equations governing the structure of neutron stars are called the Oppenheimer-Volkoff equations. They can be expressed as the following:

$$\frac{dm}{dr} = 4\pi r^2 \rho, \quad (1.9)$$

$$\frac{dP}{dr} = -\frac{\rho m}{r^2} \left(1 + \frac{P}{\rho}\right) \left(1 + \frac{4\pi P r^3}{m}\right) \left(1 - \frac{2m}{r}\right)^{-1}, \quad (1.10)$$

$$\frac{d\Phi}{dr} = -\frac{1}{\rho} \frac{dP}{dr} \left(1 + \frac{P}{\rho}\right)^{-1}, \quad (1.11)$$

where  $r$  is the local radial distance from the stellar center,  $m(r)$  the mass inside radius  $r$ ,  $\rho(r)$  the density,  $P(r)$  the pressure,  $\Phi(r)$  the gravity potential. There are three equations and four variables. If the above set of equations is supplied with the equation of state,  $P = P(\rho)$ , and the boundary conditions given at the center  $r = 0$  as  $M(0) = 0$  and  $\rho(0) = \rho_c$ , integration from the center toward the boundary yields a density profile. The radius of the neutron star is defined to be at  $r = R_0$  where  $P(R_0) = 0$ .

Unfortunately, the equation of state of matters above nuclear density is poorly

understood. Below the nuclear density, we believe that we have fairly good understanding of the equation of state through solid state physics.

### 1.2.2 Equation of State

Several models, mainly phenomenological, exist, giving quite different equations of state.

#### Below Nuclear Density

Below the nuclear density, the pressure can be expressed as  $P = P_{ion} + P_e + P_n$ , the sum of the pressures from ions, free neutrons and free electrons. When they are treated as a perfect gas, the pressures from the electrons and neutrons  $P_e$  and  $P_n$  can be calculated from the following basic equation:

$$P = \frac{1}{3} \int p v n(p) d^3 p, \quad (1.12)$$

with  $n(p)$  as particle number density and  $v = \frac{p}{m} / [1 + (p/mc)^2]^{1/2}$  relativistically, or  $v = p/m$  nonrelativistically.

If the electrons are degenerate, the number density as a function of momentum can be expressed as :

$$n(p) d^3 p = \frac{2}{h^3} \frac{4\pi p^2 dp}{\exp(\frac{E-\mu}{kT}) + 1}, \quad (1.13)$$

or for a complete degeneracy,

$$n(p) d^3 p = \begin{cases} \frac{2}{h^3} 4\pi p^2 dp & p < p_F \\ 0 & p > p_F, \end{cases} \quad (1.14)$$

where  $\mu$  is the chemical potential, which is a known function of  $\rho$  and  $T$ , and  $p_F$  is Fermi momentum. The energy  $E$  can be expressed as  $p^2/2m$  non-relativistically or  $\sqrt{p^2c^2 + m^2c^4}$  relativistically.

In the relativistically and degenerate regime:

$$\begin{aligned} P &= \frac{1}{3} \int_0^{p_F} \frac{\frac{p^2}{m}}{[1 + (\frac{p}{mc})^2]^{1/2}} \frac{2}{h^3} 4\pi p^2 dp \\ &= \frac{8\pi}{3mh^3} \int_0^{p_F} \frac{p^4 dp}{[1 + (\frac{p}{mc})^2]^{1/2}}, \end{aligned} \quad (1.15)$$

In the non-relativistically and degenerate regime,  $v = p/m$ , and the pressure is

$$\begin{aligned} P &= \frac{1}{3} \int_0^{p_F} \frac{p^2}{m} \frac{2}{h^3} 4\pi p^2 dp \\ &= \frac{8\pi}{3mh^3} \int_0^{p_F} p^4 dp \\ &= \frac{8\pi}{15mh^3} p_F^5. \end{aligned} \quad (1.16)$$

In the non-relativistic and partially degenerate regime, the pressure can be expressed as:

$$\begin{aligned} P &= \frac{1}{3} \int_0^\infty p \frac{p}{m} \frac{8\pi p^2 dp}{h^3 (\exp(\frac{E-\mu}{kT}) + 1)} \\ &= \frac{8\pi}{3mh^3} \int_0^\infty \frac{p^4 dp}{\exp(\frac{E-\mu}{kT}) + 1}. \end{aligned} \quad (1.17)$$

Note that the criterion used to judge whether the particles are relativistic or non-relativistic is (Clayton 1968)

$$\xi_r = \left( \frac{\rho}{7.3 \times 10^6 \text{ gm/cm}^3} \right) \mu_e. \quad (1.18)$$

If  $\xi_r$  is  $\gg 1$ , it is relativistic. If  $\xi_r$  is  $\ll 1$ , it is non-relativistic. The criterion for degeneracy is

$$\xi_d = \left( \frac{\rho}{2.4 \times 10^{-8}} \right) \mu_e T^{3/2}. \quad (1.19)$$

If  $\xi_d$  is  $\gg 1$  ( $\ll 1$ ), it is degenerate (non-degenerate). For  $T$  is  $< 10^9 K$ , as is the case during most of the life time of a neutron star, the criterion for the relativistic case is more strict than the criterion for degeneracy. Therefore in the extremely relativistic regions, the matter is also degenerate, and in the regions where it is partially degenerate, it is non-relativistic.

The above expressions are derived under the assumption that particles inside neutron stars are perfect gases. However, free electrons experience Coulomb forces, while free neutrons and protons experience nuclear forces. These forces affect the pressure. To calculate the corrections to the pressure caused by the interactions between the particles, we start with the basic thermodynamic equation (Shapiro & Teukolsky 1983):

$$P = P_{perfect} + n^2 \frac{\partial}{\partial n} (\varepsilon). \quad (1.20)$$

Here  $P_{perfect}$  is the pressure of an ideal gas,  $n$  is the particle number density,  $\varepsilon$  is the energy of the interactions per particle.  $\varepsilon$  can be expressed as  $\varepsilon = \varepsilon_c + \varepsilon_n$ , with  $\varepsilon_c$  as the energy due to Coulomb interaction and  $\varepsilon_n$  as the energy due to nuclear interaction. For the Coulomb interaction,  $\varepsilon_c$  can be expressed as:

$$\varepsilon_c = \varepsilon_{e-e} + \varepsilon_{e-i}, \quad (1.21)$$

where  $\varepsilon_{e-e}$  is the potential energy due to Coulomb interactions between electrons and  $\varepsilon_{e-i}$  is the potential energy due to Coulomb interactions between electrons and ions.

Suppose that the gas is divided into neutral spheres of radius  $r_0$  about each nucleus, which contains  $Z$  electrons nearby. Then  $\varepsilon_{e-e}$  and  $\varepsilon_{e-i}$  can be calculated by

$$\begin{aligned}\varepsilon_{e-e} &= \frac{1}{Z} \int_0^{r_0} \frac{q dq}{r} \\ &= \frac{3Ze^2}{5r_0},\end{aligned}\tag{1.22}$$

with  $q = Ze \frac{r^3}{r_0^3}$ , and

$$\begin{aligned}\varepsilon_{e-i} &= -\frac{1}{Z} \int_0^{r_0} \frac{Ze}{r} dq \\ &= -\frac{3Ze^2}{2r_0}.\end{aligned}\tag{1.23}$$

For nuclear interaction,  $\varepsilon_n$  can be expressed as an integral:

$$\varepsilon_n = \frac{1}{2} \int \int f(|\vec{r}_1 - \vec{r}_2|, \vec{s}_1, \vec{s}_2, \vec{L}) dV_1 dV_2,\tag{1.24}$$

where  $f(|\vec{r}_1 - \vec{r}_2|, \vec{s}_1, \vec{s}_2, \vec{L})$  is the nuclear potential between two nucleons. It is a function of the distance between these two nucleons, and spins and angular momenta of these two nucleons. A simple approximation for the nuclear potential is a Yukawa potential.

If the ions are free gases, then  $P_{ion}$  is just  $nkT$ , because the ions are too heavy to be degenerate or relativistic. If the ions solidify and form a lattice, then  $P_{ion}$  is caused by phonons and Coulomb interactions between the ions (see §2.3.1).

### Above Nuclear Density

When calculating the equation of state,  $P = P(\rho)$ , in the high density regions, the nuclear potential is required. Inside the core, the composition is primarily neutrons,

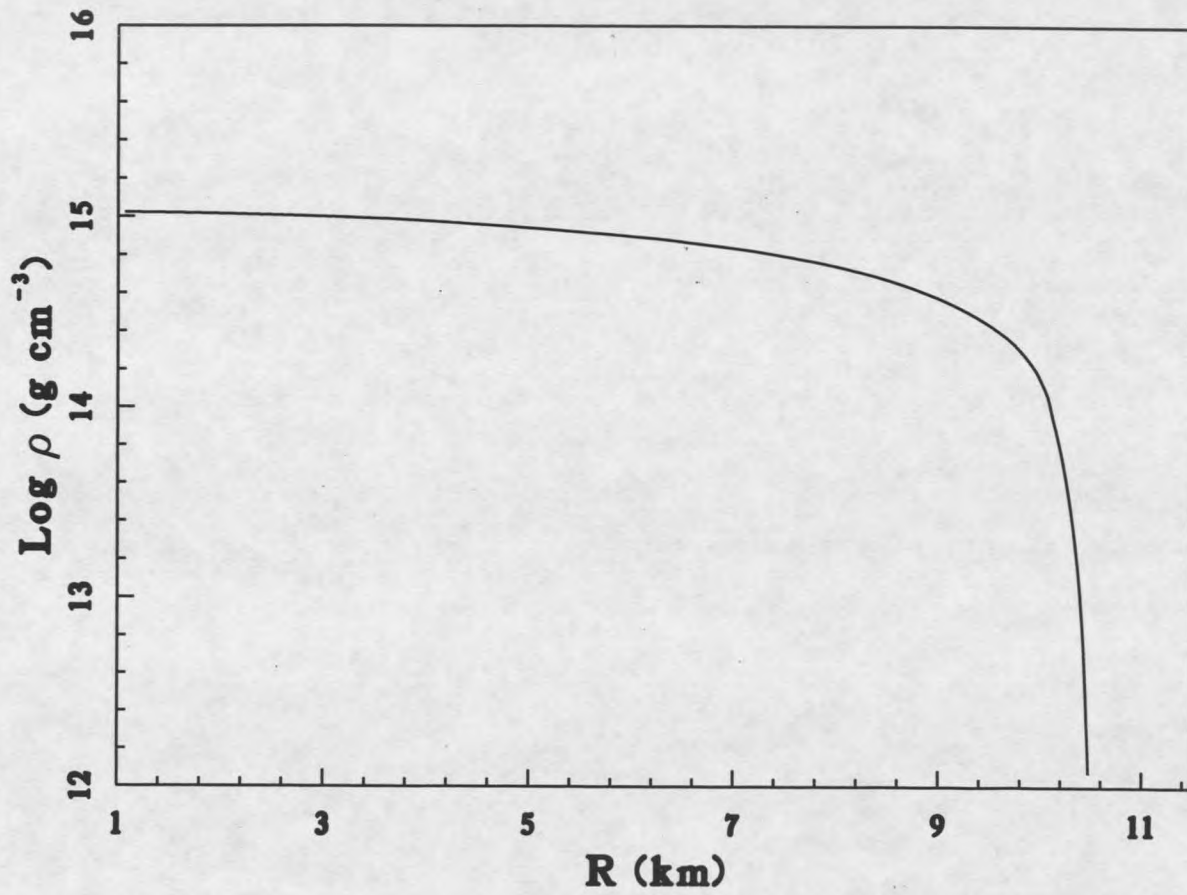
plus a small amount of protons and electrons. In the central region, the density is so high and the distance between two nucleons so short that nuclear interactions cannot be neglected. Our current knowledge about nuclear interactions are basically phenomenological, and are only tested in the regions where the density is below and near nuclear density. To extend to the regime where the density is significantly higher than nuclear density, the only way is by extrapolation. Among the theoretical alternatives for the dense matter equation of state are the FP Model, which was proposed by Friedman and Pandharipande (1981), and the Baym-Bethe-Pethick equation of state (Baym, Bethe and Pethick 1971), the BPS Model (Baym, Pethick and Sutherland 1971), and the PS Model (Pandharipande and Smith 1976), etc.

### 1.2.3 Density Profile

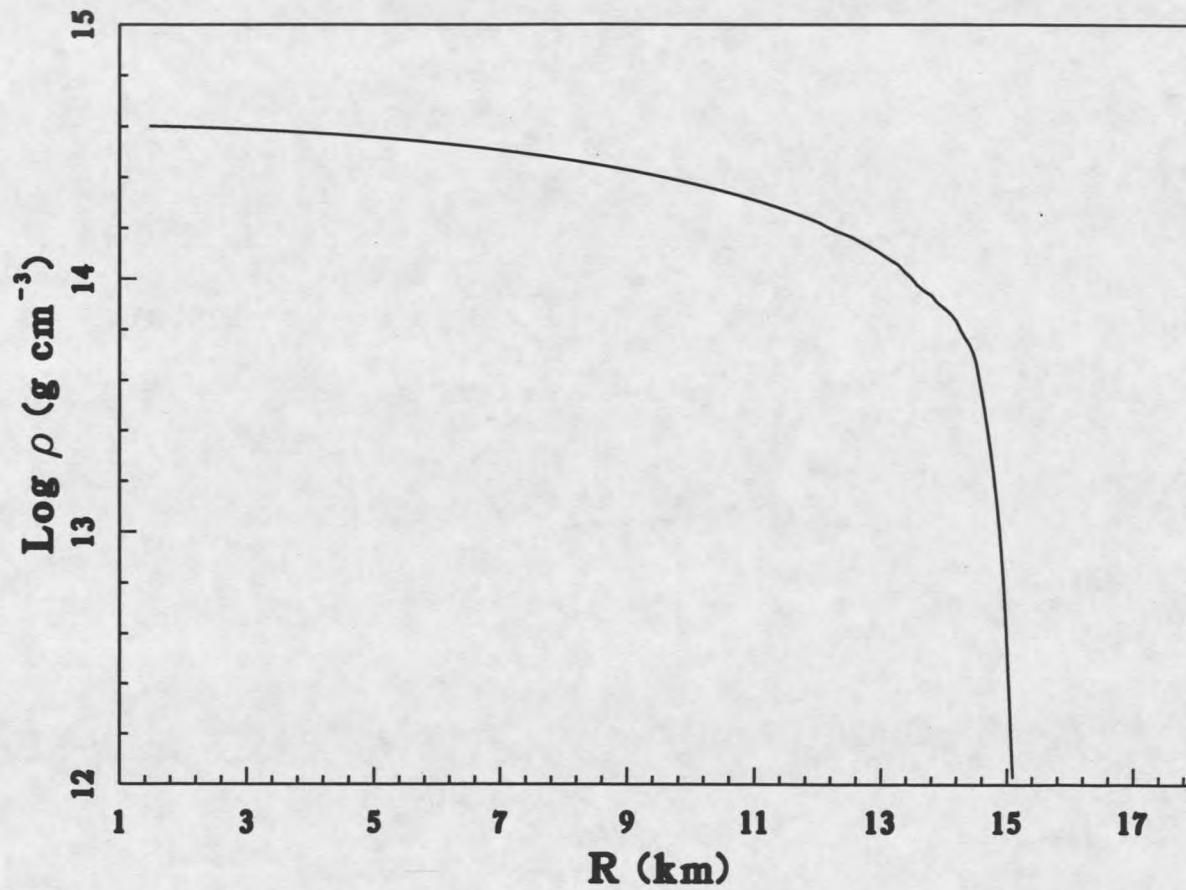
Once the equation of state is known, given an initial central pressure  $P_c$ , we can integrate the hydrostatic equations from the center outward, and obtain a structure profile. In Fig(1.1), we show the density profile for the FP Model.

Different nuclear energy potential models will give different equations of state. In Fig(1.2) and Fig(1.3), we show two neutron star structures obtained with the BPS Model and PS Model. Compared with the FP model in Fig(1.1), the BPS Model is softer, that is  $P_{BPS} < P_{FP}$  for the same value of  $\rho$ , so with the same mass, the FP Model has a larger radius, thus a lower density than the BPS Model. On the other hand, the PS Model is the stiffest among the three models, it has the largest radius and the lowest density. The FP Model is of intermediate stiffness.

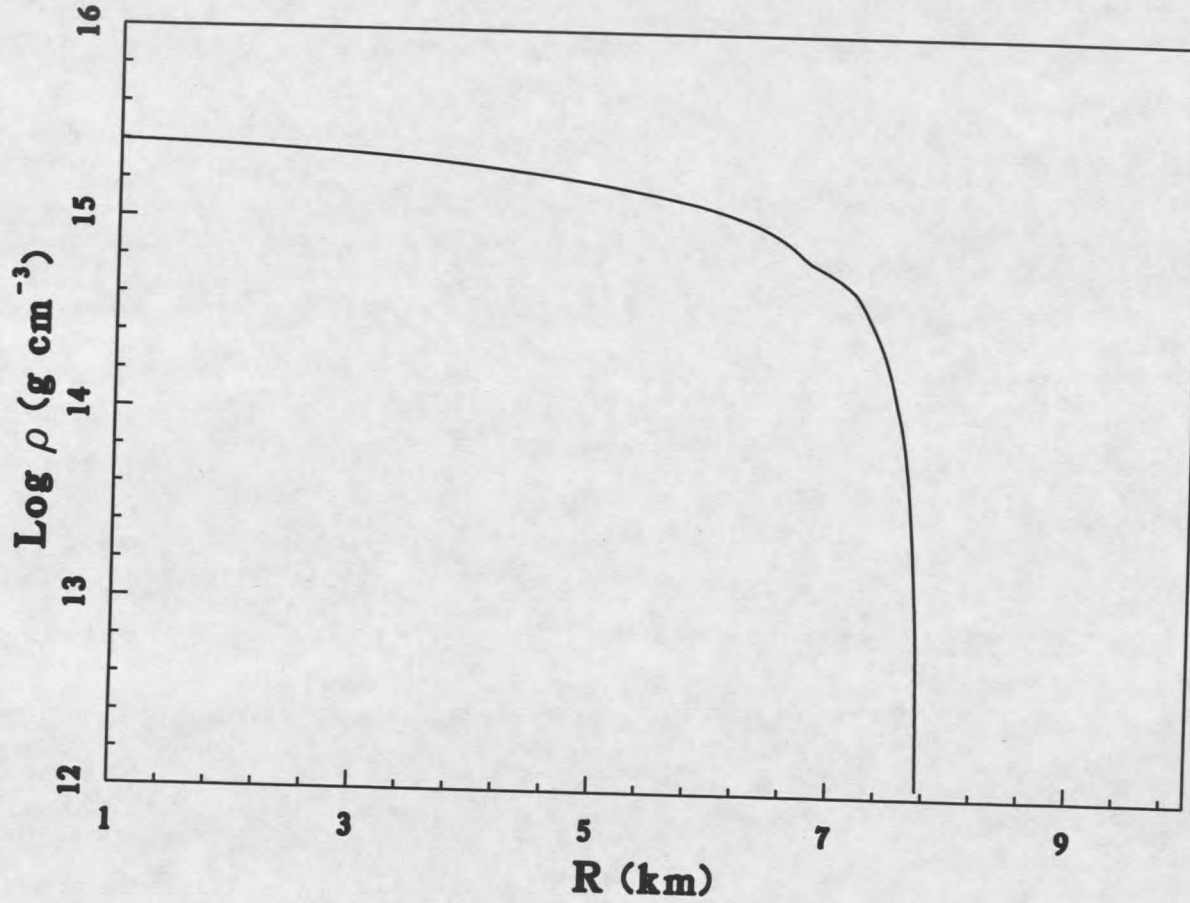
From these figures, we can see that the density is nearly constant in the interior,



**Fig(1.1) Density Profile for FP Type Neutron Stars**



**Fig(1.2) Density Profile for PS Type Neutron Stars**



**Fig(1.3) Density Profile for BPS Type Neutron Stars**

but near the surface, the density drops drastically from  $10^7 gcm^{-3}$  to zero in a region of about 1 meter thick. This region is called the envelope. The region from  $4.3 \times 10^{11} gcm^{-3}$  to the outmost envelope is called the outer crust. Above  $4.3 \times 10^{11} gcm^{-3}$ , neutron drip occurs, and a gas of free neutrons coexists with a lattice of neutron rich nuclei. The region between  $2.8 \times 10^{14} gcm^{-3}$  and  $4.3 \times 10^{11} gcm^{-3}$  is called the inner crust. Above  $2.8 \times 10^{14} gcm^{-3}$ , it is the core. Inside the core, the nuclei dissolve. The core consists mostly of neutrons and a small percentage of protons and electrons.

## 1.3 Magnetic Field and Superfluidity

### 1.3.1 Magnetic Field

In §1.1, we discussed one evidence for the existence of strong magnetic fields around neutron stars. Further evidence is provided by the 58 keV emission line from X-ray Pulsar Her X-1.

The origin of this 58 keV emission line can be understood in the following way. Suppose there is a uniform  $\vec{B}$  field. A charged particle moves inside  $\vec{B}$  with a velocity  $\vec{v}$ , which has a component  $v_0$  in the plane perpendicular to  $\vec{B}$ . The particle will move in a circular orbit due to the influence of the  $\vec{B}$  field. The velocity of the particle satisfies:

$$eBv_0 = m \frac{v_0^2}{r}, \quad (1.25)$$

which leads to:

$$r = \frac{mv_0}{eB}, \quad (1.26)$$

$r$  is the radius of the circular orbit, and is inversely proportional to the magnetic field strength  $B$ .

In the case of neutron stars, the magnetic field can exceed  $1 \times 10^{12}$  Gauss. Then, for electrons with  $m_e = 9.1 \times 10^{-31} \text{kg}$  and  $e = 1.6 \times 10^{-19} \text{C}$ , if the velocity  $v_0$  is  $c/10$ ,  $r$  would be  $\sim 10^{-11} \text{m}$ , which is comparable to the de Broglie wavelength  $\lambda$ . Thus, the quantum effects are important.

Let us redo the problem quantum-mechanically. The Lagrangian  $L$  for an electron in a magnetic field is

$$L = \frac{1}{2}mv^2 + \frac{e}{c} \vec{v} \cdot \vec{A}, \quad (1.27)$$

with  $\vec{A} = \frac{1}{2} \vec{B} \times \vec{r}$ . The momentum  $\vec{p}$  is

$$\begin{aligned} \vec{p} &= \frac{\partial L}{\partial \vec{v}} \\ &= m \vec{v} + \frac{e}{c} \vec{A} \\ &= \frac{1}{2} m \vec{v}. \end{aligned} \quad (1.28)$$

The Bohr quantization condition is

$$\oint L_\theta d\theta = nh. \quad (1.29)$$

Since  $L_\theta = \vec{P} \times \vec{r} = \frac{1}{2} mvr$ , then

$$\oint \frac{1}{2} mvr d\theta = \pi mvr = nh, \quad (1.30)$$

and because

$$r = \frac{v}{\omega_0}, \quad (1.31)$$

where  $\omega_0 = eB/m$ , we have:

$$\frac{mv^2}{\omega_0} = 2n\hbar. \quad (1.32)$$

The kinetic energy  $E$  can be expressed as:

$$E = \frac{1}{2}mv^2 = n\hbar\omega_0. \quad (1.33)$$

It is quantized, and the differences between two consecutive energy levels are

$$\Delta E = \hbar\omega_0. \quad (1.34)$$

As the electrons jump from one level to the next, photons of energy  $\hbar\omega_0$  will be emitted. If  $B = 1 \times 10^{12} \text{Gauss}$ ,  $\omega_0 = 2 \times 10^{19} \text{s}^{-1}$ , and  $\Delta E = \hbar\omega_0 \approx 10 \text{keV}$ . The  $58 \text{keV}$  photons from Her X-1 imply that the magnetic field strength is about  $5 \times 10^{12} \text{Gauss}$ . Usually the magnetic field inside neutron stars is assumed to be dipolar. The field lines of a dipolar field are shown in Fig(1.4). As the magnetic field corotates with the star, electric fields are induced. In the region that is within a radius  $R_{lc}$  from the star, where  $R_{lc} = \Omega/c$ , the magnetic field has an overwhelming influence over the charged particles. This cylindrical region within  $R_{lc}$  is called the light cylinder. The field lines 1, 2, 3 and 1', 2', 3' are closed field lines, and the field lines 0 and 0' are open.

How is the strong radiation produced on the surfaces of neutron stars? The radio emission originates from a region that is  $\sim 10$  stellar radii away from the surface. The beam is radiated by high energy particles constrained to move along the field lines over the magnetic poles. The individual radio pulses are often highly polarized indicating the presence of strong magnetic fields. The intensities of the

emitted radio emission are so high that they cannot be due to thermal emissions or incoherent synchrotron radiation, only coherent radiation can produce such high intensities. When the radiation is coherent, the total energy is proportional to  $N^2$ , not  $N$ , with  $N$  as the number density of the particles. Because the electrons are constrained to move together, they act as one particle of charge  $Ne$ . When a charged particle with charge  $q$  is accelerating, the radiated power is

$$\frac{dE}{dt} = \frac{8\pi^2}{3} \left(\frac{eB}{mc}\right)^2 \frac{v^2}{c^3} q^2. \quad (1.35)$$

For  $N$  electrons radiating noncoherently, the total energy radiated will be  $N \frac{dE}{dt}$ . If  $N$  electrons are synchronised, then the total energy radiated is

$$\begin{aligned} \frac{dE_{total}}{dt} &= -\frac{8\pi^2}{3} \left(\frac{NeB}{mc}\right)^2 \frac{v^2}{c^3} \\ &= N^2 \frac{dE_e}{dt}. \end{aligned} \quad (1.36)$$

The intensity is enhanced by  $N^2$  times.

As to understanding how charged particles are accelerating along the field lines, we need to turn to the electrodynamics of a rotating magnetic neutron star, which is a very difficult problem, as yet incompletely solved. Goldreich and Julian (1969) assumed the magnetic dipole moment is aligned with the rotating axis, and the neutron star is a good electric conductor. If the interior of a neutron star is a good conductor, then:

$$E' = 0, \quad (1.37)$$

where  $E'$  is the electric field in the rotating frame. Changing to the inertial frame,

we have inside the neutron star,

$$\vec{E} + \left( \frac{\vec{\Omega} \times \vec{r}}{c} \right) \times \vec{B} = 0, \quad (1.38)$$

where  $\vec{\Omega}$  is the angular velocity vector. Since neutron stars are good conductors, we can assume there are no currents on the stellar surfaces. Then  $\vec{B}$  inside is a static dipole field,

$$\vec{B} = \frac{B_0 R^3}{2r^3} (2\hat{r} \cos \theta + \hat{\theta} \sin \theta). \quad (1.39)$$

Substitute the expression for  $\vec{B}$  into Equation(1.38), we get:

$$\vec{E} = -\frac{B_0 R \Omega \sin \theta}{2c} (-\hat{r} \sin \theta + 2\hat{\theta} \cos \theta). \quad (1.40)$$

Integrating  $\vec{E} \cdot d\vec{r}$  from the center toward the surface, we obtain

$$\begin{aligned} \Phi_{in} &= \int_0^R \vec{E} \cdot d\vec{r} \\ &= \frac{B_0 R^2 \Omega}{2c} \sin^2 \theta + C. \end{aligned} \quad (1.41)$$

Suppose outside the star it is a vacuum. Then the Poisson Equation  $\nabla^2 \Phi_{out} = \rho$  becomes the Laplace Equation.

$$\nabla^2 \Phi_{out} = 0. \quad (1.42)$$

With the boundary conditions:

$$\begin{aligned} r \longrightarrow \infty, \quad \Phi_{out} \longrightarrow 0 \\ \text{and} \\ r = R, \quad \Phi_{out} |_{R} = \Phi_{in} |_{R}, \end{aligned} \quad (1.43)$$

we get:

$$\Phi_{out}(r, \theta) = \frac{B_0 R^5 \Omega}{2r^3 c} \left( \sin^2 \theta - \frac{2}{3} \right) + C'. \quad (1.44)$$

Is the above solution stable under the circumstance of the neutron star?

Since the electric field is so strong compared to gravity, any surface charge will be pulled off the surface by the strong electric field. As is shown below, the above solution gives a non-zero surface charge density. That indicates it is not a stable solution.

From Equation(1.39), we know  $\vec{B} \cdot \hat{r} \neq 0$  when  $\theta \neq 90^\circ$ , and

$$\vec{B} \cdot \vec{E} = 0 \quad (1.45)$$

for  $r < R$ , also

$$\vec{B} \cdot \vec{E} = -\frac{B_0^2 R^8 \Omega}{r^7 c} \cos^3 \theta \quad (1.46)$$

for  $r > R$ . Since the tangential component of the electric field is continuous,

$$\Phi_{out} |_{R=} = \Phi_{in} |_{R,} \quad (1.47)$$

then

$$\vec{E} \cdot \hat{r} |_{R-} \neq \vec{E} \cdot \hat{r} |_{R+} \quad (1.48)$$

That means there will be surface charges, which will be flowing into the vacuum until the surface charges disappear, and the interior and exterior  $\vec{E}$  field become continuous. Then Equation(1.40) for  $\vec{E}$  would apply for both the interior and exterior. The charge density outside the neutron star would be

$$\begin{aligned} \rho_e &= \frac{\nabla \cdot \vec{E}}{4\pi} \\ &= \frac{\vec{B} \cdot \vec{\Omega}}{2\pi c} \\ &= \frac{B_0 R^3 \Omega}{4\pi r^3 c} (\sin^2 \theta - 2 \cos^2 \theta). \end{aligned} \quad (1.49)$$

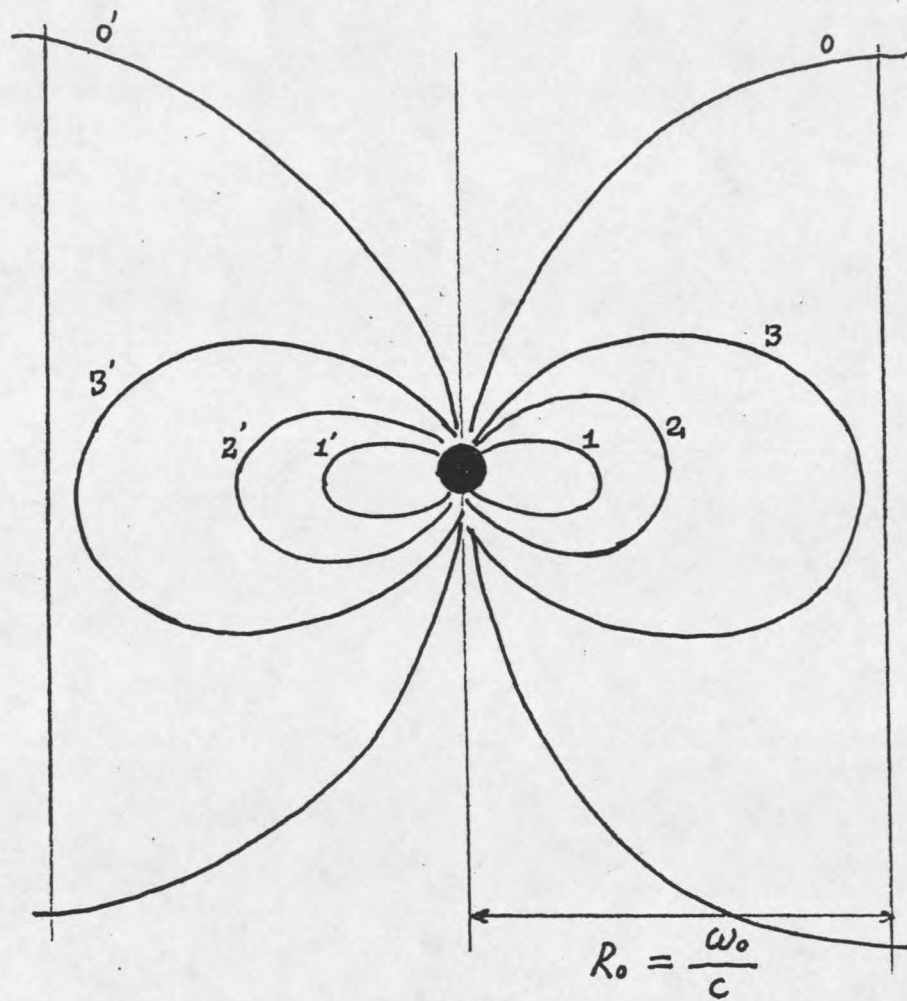
It implies a particle density of  $\sim 10^{11} \text{cm}^{-3}$ , which is very small, compared to the particle density on the surface of  $10^{20} \text{cm}^{-3}$ . A small amount of accretion of charged plasma would neutralize the charged density in the space and cause charged particles to stream out of the surface. The charged particles will move along the  $\vec{B}$  field lines. There are two kinds of  $\vec{B}$  field lines, one is open and the other is closed, as shown in Fig(1.4). When the particles are moving along the closed field lines, they will eventually come back to the stellar surface. When the particles are moving along the open field lines, they will form beamed winds.

Why is the radio radiation from the neutron stars generally pulsed? The pulsation can be understood by using a lighthouse as a model. As the pulsar rotates, the two beams radiating out of the two poles of the neutron star will sweep through the observer. Depending on the angle between the magnetic field and rotating axes, and also depending on the size of the beam, the observer may receive one or two pulses during each period.

The existence of magnetic fields affects the thermal conductivity of neutron star matters and will change the cooling rate of neutron stars. Under strong magnetic fields, the thermal conductivity becomes a tensor, the conductivities along and perpendicular to the magnetic field become different, and the cooling problem becomes a 2-dimensional problem. The cooling calculations of neutron stars with strong magnetic fields will be discussed in detail in Chapters 2 and 3.

### 1.3.2 Superfluidity

For a Bose system, when the temperature drops below the critical temperature



Fig(1.4) Illustration of a Dipolar Magnetic Field

$T_{crit}$ ,

$$T_{crit} = \frac{2\pi\hbar^2}{mk_B} \left(\frac{n}{2.612}\right)^{2/3}, \quad (1.50)$$

the system will undergo a second-order phase transition, Bose condensation, from the normal state to the superfluid state.

The number density of particles in the ground state after the Bose condensation is

$$n_T = n_0 \left[1 - \left(\frac{T}{T_{crit}}\right)^{3/2}\right]. \quad (1.51)$$

Here  $n_0$  is the total number density of the particles. If  $T \sim 0.1T_{crit}$ , then  $n_T \sim n_0$ , so most of the particles are in the ground state when T is lower than the critical temperature. Because friction is caused by momentum transfer between particles, we expect the friction to disappear when the particles are in the same state.

For a system of fermions, if there are attractive interactions between them, under certain conditions, fermions can pair and form bosons. When the temperature is low enough, Bose condensation can be realized in a Fermi system too. These pairs of fermions are called the Cooper Pairs. Below we give a brief explanation of how the Cooper pairs can form. The idea is from Baym (1973).

Let H be the Hamiltonian of two fermions with the attractive interaction,

$$H = \frac{p_1^2}{2m} + \frac{p_2^2}{2m} + V, \quad (1.52)$$

where V is non-positive, because of the attractive nature of the interaction. Let  $|\phi\rangle$  be the wave function of this two-fermion system. The Schrödinger equation is

$$H|\phi\rangle = E|\phi\rangle. \quad (1.53)$$

Consider two electrons outside the fermi surface. Between these two electrons, when their momenta are within a certain range above the fermi sea, i.e when their momenta are larger than the fermi momentum  $p_f$  and smaller than  $p_a$ , with  $p_a$  as a momentum slightly higher than  $p_f$ , there will be a weak attractive force between them. This kind of attractive force is caused by the attractive Coulomb forces between the ions and the two electrons.

For two free electrons, the total wavefunction is simply:

$$\Psi(\vec{r}_1, \vec{r}_2, t) = \frac{e^{i\vec{k}_1 \cdot \vec{r}_1}}{\sqrt{L^3}} e^{-i\frac{\epsilon_{k_1}}{\hbar} t} \cdot \frac{e^{i\vec{k}_2 \cdot \vec{r}_2}}{\sqrt{L^3}} e^{-i\frac{\epsilon_{k_2}}{\hbar} t}, \quad (1.54)$$

with  $L^3$  as the total volume and  $k_i = p_i/\hbar$ . The wavefunction of these two weakly interacting electrons can be written as a sum of the wavefunctions of two non-interacting electrons.

$$\Psi(\vec{r}_1, \vec{r}_2, t) = \sum_{\vec{k}_1, \vec{k}_2} a_{\vec{k}_1, \vec{k}_2} \frac{e^{i\vec{k}_1 \cdot \vec{r}_1}}{\sqrt{L^3}} \frac{e^{i\vec{k}_2 \cdot \vec{r}_2}}{\sqrt{L^3}} e^{-i\frac{E}{\hbar} t}. \quad (1.55)$$

Here  $E$  is the total energy of the two-fermion system. The Schrödinger equation then becomes

$$\left( \frac{p_1^2}{2m} + \frac{p_2^2}{2m} + V(p_1, p_2) \right) \sum_{p'_1, p'_2} a_{p'_1, p'_2} |p'_1 p'_2\rangle = E \sum_{p'_1, p'_2} a_{p'_1, p'_2} |p'_1 p'_2\rangle. \quad (1.56)$$

By multiplying both sides by  $\langle p_1 p_2 |$  and summing over  $p_1$  and  $p_2$ , we get:

$$\sum_{p_1, p_2} a_{p_1, p_2} \left[ \frac{p_1^2 + p_2^2}{2m} - E \right] + \sum_{p'_1, p'_2} a_{p'_1, p'_2} \sum_{p_1, p_2} \langle p_1 p_2 | V(p_1, p_2) | p'_1 p'_2 \rangle = 0. \quad (1.57)$$

Assume  $V(x) = -V_0 \delta(x)$ , then  $V(p_1, p_2) = -V_0$ . So:

$$\sum_{p'_1, p'_2} a_{p'_1, p'_2} \sum_{p_1, p_2} \langle p_1 p_2 | V(p_1, p_2) | p'_1 p'_2 \rangle = -V_0 \sum_{p'_1, p'_2} a_{p'_1, p'_2} \quad (1.58)$$

Substitute Equation(1.58) back into Equation(1.57), and we get:

$$\sum_{p_1 p_2} \frac{p_1^2 + p_2^2}{2m} - E = V_0, \quad (1.59)$$

or

$$1 = \sum_{p_1 p_2} \frac{V_0}{\frac{p_1^2 + p_2^2}{2m} - E}. \quad (1.60)$$

The equation (1.60) is a condition to determine the possible eigenvalues of the total energy  $E$ . Notice that  $p_1$  and  $p_2$  are restricted to have values between  $p_f$  and  $p_a$ . Given a total momentum  $p = p_1 + p_2$ , with each possible  $\varepsilon_{p_1} + \varepsilon_{p_2}$  when  $p_f < p_1, p_2 < p_a$ , Equation(1.60) has a pole. Let  $f(E) = -\sum_{p_1 p_2} V_0 / (\frac{p_1^2 + p_2^2}{2m} - E)$ , Fig(1.5) gives a graphic solution of  $f(E)$ . From Fig(1.5), we can see that the ground state of the paired fermions is lower than the simply degenerate state  $2\varepsilon_f$ . The ground state energy  $E_{GS}$  can be approximated by:

$$E_{GS} \approx 2E_F - 2\Delta, \quad (1.61)$$

where  $\Delta = E_F \exp[-2/(g_0 V_0)]$  with  $g_0 = (L^3/4\pi^2)[(2m)^{2/3}/h^3]\sqrt{E_F}$ . When the fermions pair up, they form bosons. If the temperature is sufficiently low, i.e. lower than the critical temperature of the boson system, Bose condensation will take place, and the superfluidity will appear. If the particles have charges, the superfluidity implies superconductivity.

In the central interior region of neutron stars where the density is above  $2 \times 10^{14} \text{ gm/cm}^3$ , the corresponding fermi temperature is  $10^{12} \text{ K}$ , while the actual temperature is around  $10^9 \text{ K}$ , far lower than the fermi temperature. The theoretical





































































































































































































































































































































































































